RSC Advances

PAPER

View Article Online
View Journal | View Issue

Cite this: *RSC Adv.*, 2021, **11**, 3049

Synthesis and characterization of bipyridine cobalt(II) complex modified graphite screen printed electrode: an electrochemical sensor for simultaneous detection of acetaminophen and naproxen

Tahere Kondori,[a] Somayeh Tajik,*[b] Niloufar Akbarzadeh-T,*[a] Hadi Beitollahi,[c] Cloudia Graiff,[d] Ho Won Jang*[e] and Mohammadreza Shokouhimehr*[e]

The new Co(II) compound $[Co(5,5'\text{-dmbpy})_2(NCS)_2]$ (**a1**) was prepared by reacting $Co(NO_3)_2 \cdot 6H_2O$, 5,5′-dimethyl-2,2′-bipyridine ligand, and Na(SCN). The nano-scale size of $[Co(5,5'\text{-dmbpy})_2(NCS)_2]$ (**a1**) was synthesized using sonochemical process. The size of the nanoparticles (**a2**) was ~13 ± 2 nm. We have also provided a new platform of electrochemical sensing for simultaneous detection of acetaminophen and naproxen using (**a2**) surface modified graphite screen printed electrode (SPE) in 0.1 M phosphate buffer solution (PBS, pH 7.0). In contrast to bare SPE, the modified SPE could significantly improve the electrooxidation activity of acetaminophen along with the rise in the current of an anodic peak. The peak currents acquired using differential pulse voltammetry (DPV) raised linearly with the raising of acetaminophen concentration and the sensor had a detection range over the concentration range of 0.009–325.0 μM, with a detection limit of 5.0 nM (S/N = 3). In the case of naproxen peak, currents of naproxen oxidation at the modified SPE were linearly dependent on the naproxen amounts in the range of 1.0–500.0 μM. The detection limit (S/N = 3) was calculated to be 0.03 μM. The DPV responses show that the peaks of acetaminophen and naproxen oxidation were vividly separated from one other with a potential difference of 410 mV between them. The low detection limit, high sensitivity, and stability made the relevant electrode applicable for the analysis of acetaminophen and naproxen in real samples. Further, its practical applicability was reliable and desirable in the analysis of pharmaceutical compounds and biological fluids. The benefits of using this modified electrode for the determination of analytes are compared with other works in the manuscript.

Received 26th September 2020
Accepted 27th December 2020

DOI: 10.1039/d0ra08126d

rsc.li/rsc-advances

1. Introduction

Pharmaceutical analysis plays an important role in human health.[1] Notably, their administration to a living organism helps the body to stay healthy. In general, pharmaceutical compounds are used to cure the diagnosed illnesses with biological efficacy in the body of the patients. Analytical measurements are very necessary after administration to the patients for bioavailability testing and evaluating their effectiveness and investigation of the needed dosage of drug formulation.[2] While different analytical methods including spectrophotometry, spectrofluorometer, chemiluminescence, capillary zone electrophoresis, and chromatography[3–7] have been extended for this purpose, electrochemical techniques have been considered as sensitive and cost-efficient method that can be accurately and rapidly used for pharmaceutical tests.[8–10] Compared to other analytical techniques, the electrochemical determination has been indicated to be very sensitive with less interference from non-electroactive compounds for the investigations of a wide range of pharmaceutical factors.[2,11,12]

Acetaminophen has been widely used in pharmaceuticals and it is mostly demonstrated in treatments of analgesic and antipyretic.[13] In addition, it has reliable properties for relieving pain associated with backache, headache, reducing fevers, and postoperative pain.[14] Acetaminophen can be administered in different forms (*e.g.*, tablets, capsules, and suspension).[15] Furthermore, acetaminophen is a multipurpose drug that can

[a]*Department of Chemistry, University of Sistan and Baluchestan, P.O. Box 98135-674, Zahedan, Iran. E-mail: n.akbarzadeh@chem.usb.ac.ir*

[b]*Research Center of Tropical and Infectious Diseases, Kerman University of Medical Sciences, Kerman, Iran. E-mail: tajik_s1365@yahoo.com*

[c]*Environment Department, Institute of Science and High Technology and Environmental Sciences, Graduate University of Advanced Technology, Kerman, Iran*

[d]*Department of Chemistry, Life Sciences and Environmental Sustainability, University of Parma, Parco Area delleScienze 17/A, 43124 Parma, Italy*

[e]*Department of Materials Science and Engineering, Research Institute of Advanced Materias, Seoul National University, Seoul 08826, Republic of Korea. E-mail: hwjang@snu.ac.kr; mrsh2@snu.ac.kr*

be available with significant concentration in biological compounds, in water bodies including wastewater of manufactures and unit's pharmaceuticals, as well as, considerable attention is essential for the quantification and detection of acetaminophen.

Naproxen is a compound antipyretic and anti-inflammatory applied in the treatment of nonrheumatic inflammation, migraine, and gout. Also, this drug is effective in reducing the pain of muscle cramps, muscle stiffness, and orthopedic surgery. The naproxen drug should be given with precaution in elderly patients and patients with hemophilia, gastrointestinal bleeding, and platelet coagulation dysfunction.[16] The combination of acetaminophen and naproxen their effect has been proven in the treatment of ache and has their clinical utilization validated.[17] Moreover, therapy through a combination of acetaminophen and naproxen drugs for sufferers with rheumatoid arthritis.[18,19] Consequently, developing a sensitive, selective, and simple technique for designation of acetaminophen and naproxen is required in formulations of pharmaceutical in biological fluids.

Because the electrochemical determination of biological and pharmaceutical compounds is not generally possible with conventional electrode due to overvoltage, the electrodes are modified with various compounds.[20–23] In addition, simultaneous determination of pharmacological and biological compounds on the surface of conventional electrodes is not easily achievable due to the overlap of their peaks. Therefore, more attention for extending an electrochemical sensor has been paid to modification of the materials on the surface of the electrode.[24–27]

In recent years, nanocomplexes are shown to be very effective in catalyzing the electrochemical reactions, resulting in a decrease in overpotentials and an increase in peak currents. Complexes of transition metals are particularly interesting as modifiers to catalyze the electrooxidation of some chemical and biologically important compounds due to their electrocatalytic properties, simultaneously functioning as active sites to accelerate chemical transformations and electron transfer.[28–31]

A SPE is a good electrode due to its mass production, cheap and current of low background. It can dominate electrodes of carbon paste and electrodes of shortcomings of glassy carbon,[32] containing effects of memory and operations of tedious cleaning. Moreover, the intrinsic disadvantages of SPEs including low sensitivity and repeatability decrease these electrodes' application and yet the surface of electrodes is prone to modify various sensing samples to achieve alright detection performance.[33,34]

In this work, $[Co(5,5'\text{-dmbpy})_2(NCS)_2]$ (**a1**) was synthesized and characterized by various techniques. The cobalt nanocomplex (**a2**) was prepared by the sonochemical process. The synthesized nanocomplex (**a2**) was used to surface modification of the SPE and employed in the simultaneous detection of acetaminophen and naproxen. The advantages of this modified electrode for the determination of analytes are compared with other works in the manuscript.

2. Experimental

2.1. Chemicals and characterization

The chemicals and solvents were used without further purifications from the company of Aldrich. The spectrum of FT-IR of complex (**a1**) was recorded as 1% dispersions by using a spectrometer of Shimadzu-470 by a disk of CsI and in the range of (4000–250 cm^{-1}). The spectrum of UV-Vis has resulted in a spectrometer of Shimadzu 2100. X-ray powder diffraction (XRD) calculations were conducted *via* an X'pert diffractometer from Philips Co. The scanning electron microscopic (SEM) was applied to distinguish the samples. Results of X-ray diffraction for complex (**a1**) were obtained at 173 K on a diffractometer of Bruker Apex II single-crystal, working with Mo-Kα graphite monochromatic radiator (Kα = 0.71073 Å) and have an area detector. The result of the raw frame was carried out by software of SAINT, and the rectification for absorption was made by the program of SCALE implemented in the SAINT package to obtain the data file of reflection. The structure of the sample was obtained *via* direct techniques with SHELXS-97 and refined against F2 with SHELXL-2014/7 by parameters of anisotropic thermal for all non-hydrogen atoms. The atoms of hydrogen were placed in the positions of ideal geometrical positions. The results crystallographic for complex (**a1**) were verified with the Cambridge Crystallographic Data Center.

The measurements of electrochemical were carried out with a device in the name of Autolabpotentiostat/galvanostat (PGSTAT 302N, Eco Chemie, the Netherlands). The conditions of the test under revenue control with a software of General Purpose Electrochemical System (GPES). The electrode of screen-printed (DropSend, DRP-110, Spain) contains three segments of importance, which consists of a silver pseudo-reference electrode, a graphite counter electrode, and a graphite working electrode. pH was measured by a Metrohm 710 pH meter. All experiments were performed in accordance with the guidelines Kerman University of Medical Sciences, Kerman, Iran. Informed consents were obtained from human participants of this study (Urine samples).

2.2. Synthesis of the compound (a1)

The value of 0.34 mmol of ligand 5,5′-dmbpy and 0.340 mmol of Na(SCN) was dissolved in a mixture of H_2O-methanol, then added to the value of 0.170 mmol of a solution of $Co(NO_3)_2 \cdot 6H_2O$, and mixed up at 60 °C for 2 h. The final solution slowly evaporates and crystals of the synthesized compound have been obtained, yield: 58.8%.FT-IR (CsI): 3421w ν(O–H), 2920s ν(C–H) aliphatic, 2090m ν(C=N), 1631m ν(C=C), ν(C=N), 850m ν(C=S), 827s, 662 s δ(C=C=C), δ(C=C=N), 267m ν(Co–N).[35,36] Anal. calc.: C, 57.00; H, 4.38; N, 15.33; found: C, 56.76; H,4.01; N, 15.81.

2.3. Synthesis of nanocomplex (a2)

A high-density ultrasonic probe was immersed directly into a methanol solution (10 mL) of $Co(NO_3)_2 \cdot 6H_2O$ (0.170 mmol), a proper volume of 5,5′-dmbpy (0.34 mmol) in methanol solution (20 mL) was added dropwise. The solution of NaSCN (0.34

Table 1 Selected crystallographic data and details of structure refinement for compound (**a1**)

Compound	**a1**
Formula	$C_{26}H_{24}CoN_6S_2$ 1/8H_2O
Molecular weight	545.81
Crystal system	Triclinic
Space group	$P\bar{1}$
a [Å]	9.720(4)
b [Å]	16.984(7)
c [Å]	18.625(8)
V [Å^3]	2632.7(18)
Z	4
h,k,l max	23,23,20
μ [cm^{-1}]	0.837
Refined parameters	643
R_1 [$I > 2\sigma(I)$]	$R_1 = 0.0452$
	w$R_2 = 0.1047$
wR_2 [all data]	$R_1 = 0.0862$
	w$R_2 = 0.1249$
GOF	0.947
CCDC	1888105

mmol) in 10 mL methanol was added gradually. The solution was then irradiated for 20 min with a power of 100 W. The obtained precipitates were filtered and dried in the air. The nanocomplex (**a2**): yield, 67.3%. Anal. calc. C, 57.2; H, 4.21; N, 15.73. Found: C, 57.7; H, 4.47; N, 14.95. FT-IR (CsI, cm^{-1}): 3401 (w), 3003 (s), 2085 (w), 1623(s), 842 (s), 818 (s), 657 (s), 260 (s).

2.4. Surface modification of the screen printed electrodes

The SPEs were modified by being coated with nanocomplex (**a2**). The general procedure for this involved dispersing 1 mg of nanocomplex (**a2**) in water (1 mL) for 45 min under sonication. Next 5 μL of the mixture was added to the SPE and it was placed to dry in conditions of environmental.

2.5. Preparation of real samples

Urine samples were stored in the refrigerator after collection. To start the analyses, typically, 10 mL of each compound was taken and then centrifuged at 2000 rpm for a quarter. The supernatant then passed through a 0.45 μm filter. Next various quantities of the treated urine samples were taken and placed in a flask (25 mL) and watery by a phosphate buffer solution (PBS) (pH = 7.0).

Table 2 Bond distances (Å) and bond angle (°) for complex (**a1**)

Bond length (Å)	Bond	Angle (°)	Bond angle
1.339(4)	C1 N1	124.9	N1 C1 C2
0.9300	C1 H1	115.3(3)	C4 C2 C1
1.386(5)	C1 C2	109.5	C2 C3 H3A
1.625(4)	C25 S1	109.5	H3A C3 H3
1.151(4)	C25 N5	124.3(3)	N4 C24C2
2.139(3)	N1 Co1	165.48(12)	N6 Co1 N3
2.078(3)	N5 Co1	96.15(13)	N11 Co2 N12
2.167(3)	N10 Co2	168.93(12)	N11 Co2 N8

To these compounds, different quantities of acetaminophen and naproxen were spiked.

Five 325 mg acetaminophen tablets (Amin Co., Iran) were ground and homogenized. Next, 325 mg of this powder was dissolved in PBS (25 mL) under sonication, and various quantities of this solution were added to the 25 mL volumetric flask before dilution with PBS (pH = 7.0).

Five 250 mg naproxen tablets (Chemidarou Co., Iran) were ground and homogenized. Next, 250 mg of this powder was dissolved in 25 mL of PBS in condition sonication, and various quantities of this solution were added to the 25 mL volumetric flask before dilution with PBS (pH = 7.0).

3. Results and discussion

The reaction of ligands of 5,5′-dmbpy and Na(SCN) with a salt of Co(II) (with the ratio of 2 : 2:1 molar for preparing compound

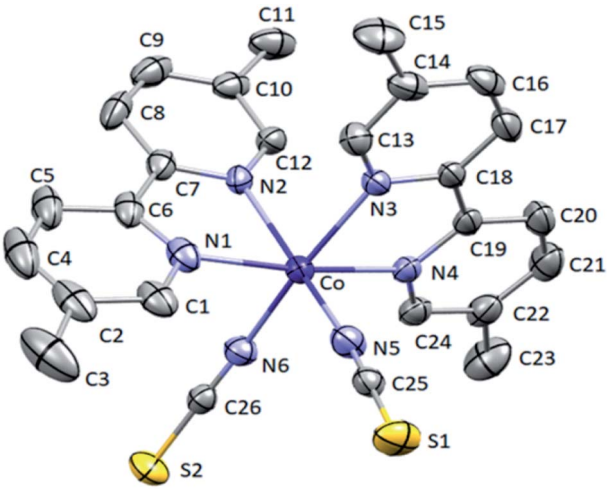

Fig. 1 ORTEP view of complex (**a1**).

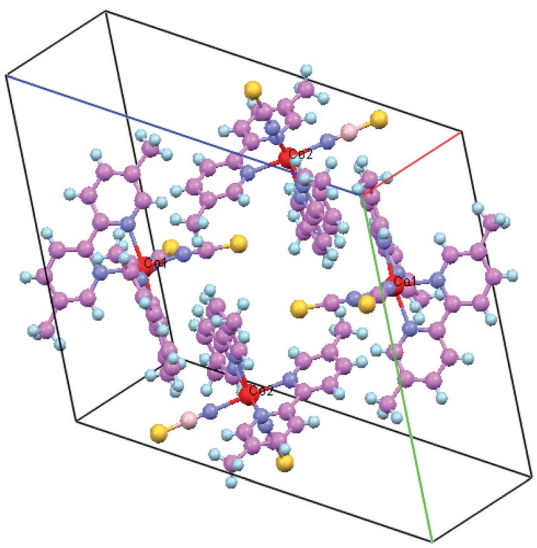

Fig. 2 Crystal packing diagram of [Co(5,5′-dmbipy)$_2$(NCS)$_2$] (**a1**).

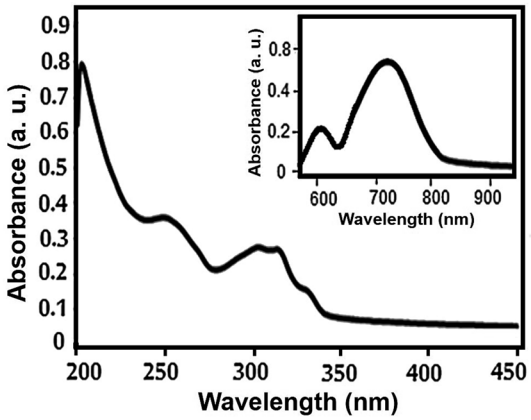

Fig. 3 UV-Vis spectrum of complex (**a1**) in methanol.

(**a1**)) in H_2O-methanol at 298 K made $[Co(5,5'\text{-dmbpy})_2(NCS)_2]$ (**a1**) complex. The compound (**a1**) was identified using spectroscopies of FT-IR, UV-Vis, and elemental analysis (CHN).

3.1. Characterization of the synthesized complex

3.1.1. Crystallographic data collection and structure determination. The compound of $[Co(5,5'\text{-dmbpy})_2(NCS)_2]$ is a stable insoluble and solid phase. Suitable crystal of titled complex for X-ray diffraction studied was synthesized by slow evaporation in methanol solution. Crystalline data of complex (**a1**) is shown in Table 1. Bond distances (Å) and bond angles (°) for complex (**a1**) are displayed in Table 2.

Oak Ridge Thermal Ellipsoid Plot (ORTEP) view and crystal packing related to complex (**a1**) are shown in Fig. 1 and 2, respectively. In this compound, Co(II) atoms are six-coordinated in distorted octahedral configurations by four N atoms from two 5,5′-dmbpy and two terminal N atoms from NCS ligands.

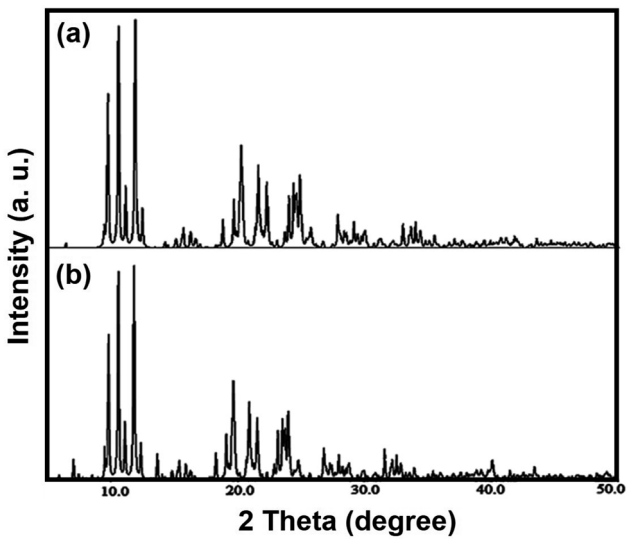

Fig. 4 XRD patterns of (a) $[Co(5,5'\text{-dmbipy})_2(NCS)_2]$ (**a1**) and (b) nanocrystals (**a2**).

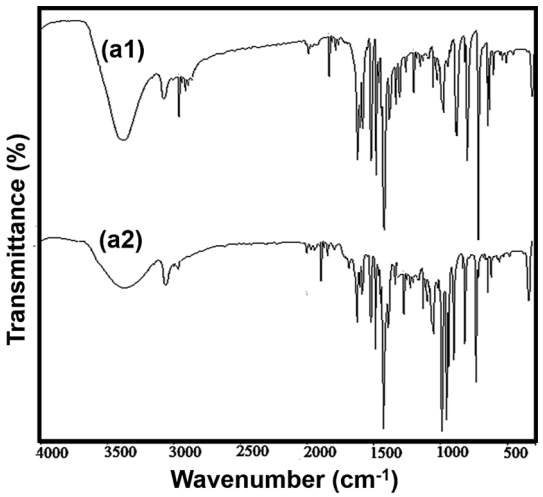

Fig. 5 FT-IR spectra of (a) $[Co(5,5'\text{-dmbipy})_2(NCS)_2]$ (**a1**) and (b) nanocrystals (**a2**).

3.1.2. Electronic absorption spectroscopy. UV-Vis spectrum of complex (**a1**) in methanol solution contains different peaks related to the transitions of ligands and Co(II) ion (Fig. 3). In the ultraviolet region, the bands at 308–317 nm, assigned to π–π* and n–π* transition of 5,5′-dmbpy ligand, respectively.[37–39] The 330 nm band is related to π–π* transition of NCS ligand which has been overlapped with the transitions of 5,5′-dmbpy ligand. The peaks at 609 and 720 nm can be relevant to $^2E_g \rightarrow {}^2T_{1g}$ and $^2E_g \rightarrow {}^2T_{2g}$ that has been related to d–d transitions of Co(II) ion.[40]

3.2. Characterization of the synthesized nanocomplex

3.2.1. X-ray powder diffraction investigation. Fig. 4 displays the replicated XRD pattern from single-crystal X-ray data of (**a1**), compared to the XRD pattern, assembled *via* a sonochemical procedure of nanocrystals of (**a2**). Sufficient agreement with minor variations in 2θ was evident among the replication and experimented X-ray diffraction patterns.

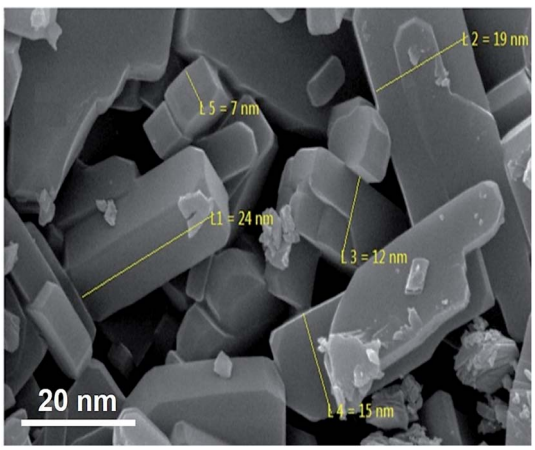

Fig. 6 SEM image of nanocrystal (**a2**).

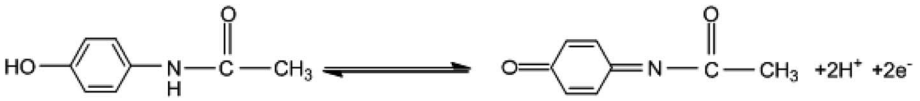

Scheme 1 Probable oxidation mechanism for acetaminophen.

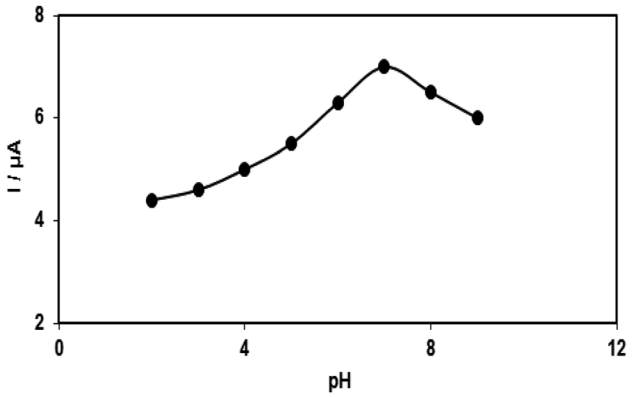

Fig. 7 Plot of I_p *vs.* pH obtained from DPVs of modified SPE in a solution containing 100.0 µM acetaminophen in 0.1 PBS with different pHs (2.0, 3.0, 4.0, 5.0, 6.0, 7.0, 8.0 and 9.0).

3.2.2. FT-IR spectrum. FT-IR spectra of complex (**a1**) and nanocrystals (**a2**) shown in Fig. 5 are related to C–H stretching vibrations of phenyl and pyridine rings and methyl groups. Several bands are evident within the 2000 to 1400 cm^{-1} range which was assigned to ν(C=N) and ν(C=C) vibrations. The medium to strong vibrational bands within the 1114 to 670 cm^{-1} region are accredited to malformation vibrations of δ(C=C=N) and δ(C=C=C) in the phenyl and pyridine rings. The band at 850 cm^{-1} is atributad to ν(C=S) vibration. The

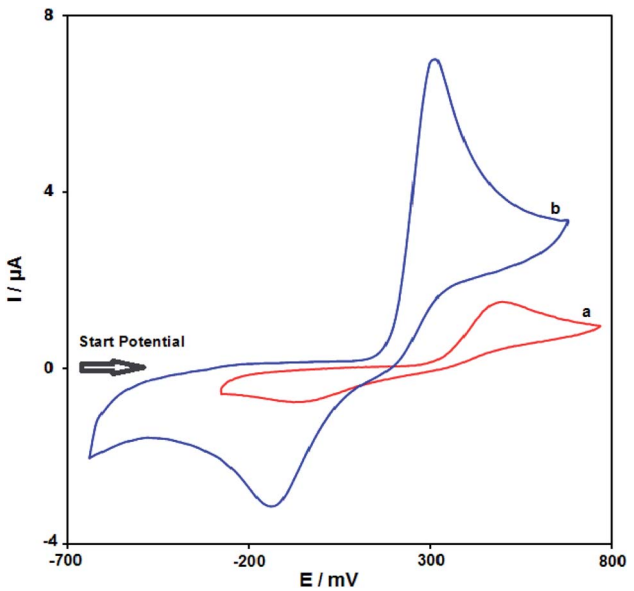

Fig. 8 Cyclic voltammograms of (a) unmodified SPE and (b) modified SPE in 0.1 M PBS (pH 7.0) in the presence of 100.0 µM acetaminophen at the scan rate 50 mV s^{-1}.

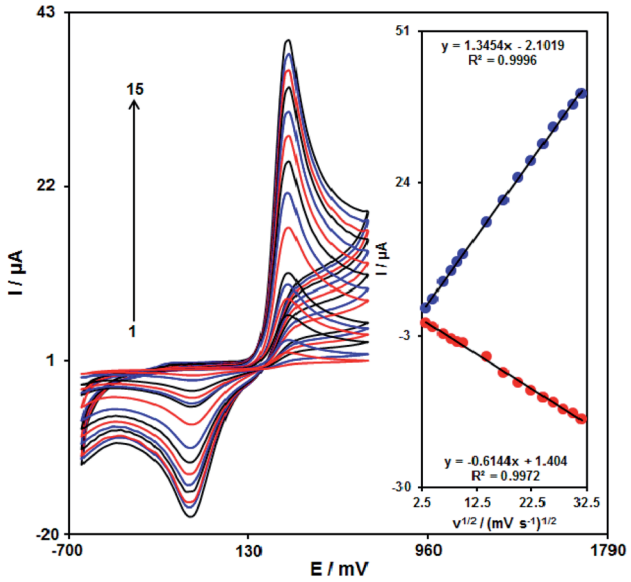

Fig. 9 Cyclic voltammograms of modified SPE in 0.1 M PBS (pH 7.0) including 100.0 µM acetaminophen at different scan rates; curves 1–15 related to 10, 20, 40, 60, 80, 100, 200, 300, 400, 500, 600, 700, 800, 900, and 1000 mV s^{-1}, respectively. Inset: variation of anodic and cathodic peak current *versus* $\nu^{1/2}$.

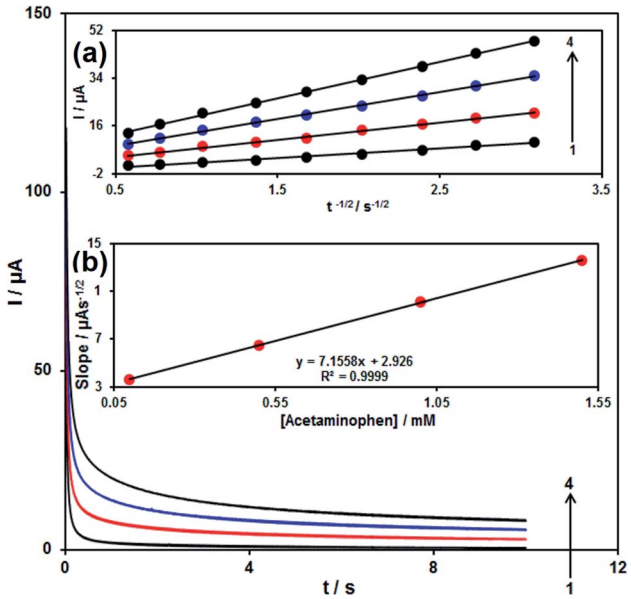

Fig. 10 Chronoamperograms measured at modified SPE in 0.1 M PBS (pH 7.0) for a various concentrations of acetaminophen material. The curves 1–4 related to 0.1, 0.5, 1.0, and 1.5 mM of acetaminophen. Insets: (a) plots of *I vs.* $t^{-1/2}$ calculated from chronoamperograms 1–4. (b) The plot of the straight lines slope *versus* acetaminophen concentration.

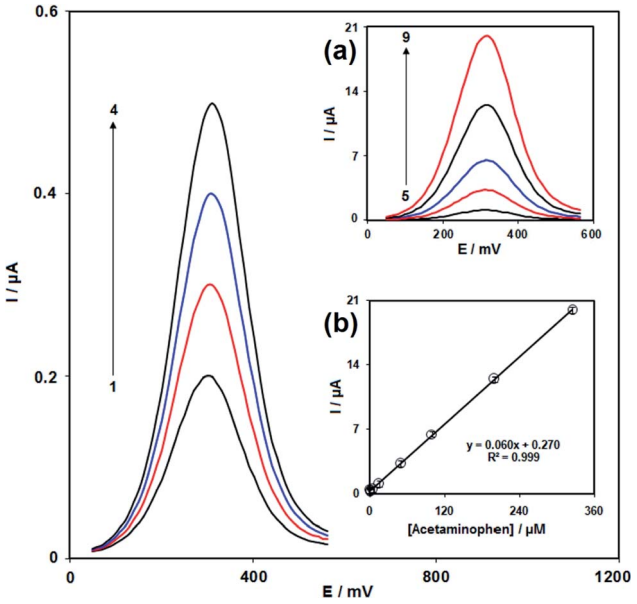

Fig. 11 DPVs of modified SPE in 0.1 M (pH 7.0) including various concentrations of acetaminophen (0.009, 0.05, 0.5, and 5.0 μM. Inset (a): DPVs of modified SPE for the curve related to 15.0, 50.0, 100.0, 200.0, and 325.0 μM of acetaminophen. Inset (b): plot of the current of peak like a function of concentration of acetaminophen material approximately in the 0.009–325.0 μM.

stretching vibration bond of Co–N was evident at 267 cm^{-1}. According to the FT-IR spectrum of the complex (**a1**), the similarities to the FT-IR spectrum of single-crystalline substances are evident (Fig. 5).[35,36]

3.2.3. Microscopy. SEM photograph of (**a2**) displays the synthesized nanoparticles having uniform morphology (Fig. 6). The size of the particle obtained by using the SEM method was ~13 ± 2 nm for the titled compound.

3.3. Electrochemical analysis

3.3.1. Electroanalysis of acetaminophen using various electrodes. It is clear that the electrochemistry of acetaminophen is correlated to pH of the media (Scheme 1). Therefore, optimization of the pH is very important in the electroanalysis of acetaminophen drug. Accordingly, the functional of electrochemical of acetaminophen was in 0.1 M PBS with various pH in the range of 2.0–9.0 were evaluated *via* the nanocomplex (**a2**) SPE (Fig. 7). The results showed using the modified SPE, the reaction favored pH of 7.0 and therefore neutral pH was used in all of the tests.

Fig. 8 illustrates the cyclic voltammograms recorded for 100.0 μM solution of acetaminophen using an unmodified SPE (curve a) and modified SPE (curve b). With the help of the modified electrode, the oxidation peak potential of acetaminophen was observed at 300 mV at a modified SPE, whereas the corresponding peak was observed at 500 mV at an unmodified SPE. The anodic peak current at the former is 460% higher than that at the latter, indicating a positive influence of modification.

3.3.2. Influence of scan rate. The relation between the potential scan rate and the electrooxidation current of acetaminophen was evaluated and based on the results (Fig. 9) raising the rate of scan was found to increase the current. Given the linear relationship among the square root of the scan rate ($\nu^{1/2}$) and the anodic and cathodic peak currents (I_p), it was deduced which the process of oxidation and reduction named diffusion-controlled phenomenon for acetaminophen.

3.3.3. Chronoamperometry tests. Modified SPE was also used for the chronoamperometric analysis of various amounts of acetaminophen in PBS (pH = 7). The analyses were performed by applying a potential of 350 mV to the working electrodes (Fig. 10). The chronoamperometric current for an electroactive sample that has a diffusion coefficient of D, under mass-transport controlled situations is given using Cottrell's equation:[41]

$$I = nFAD^{1/2}C_b\pi^{-1/2}t^{-1/2} \quad (1)$$

where I is current (A), D is the diffusion coefficient ($cm^2\ s^{-1}$), C_b is the bulk concentration of an analyte (mol cm^{-3}), A is the surface area of the electrode (cm^2), F is Faraday's constant, t is

Table 3 A comparison of the efficiency of modified SPE in this work and various modified electrodes reported for the detection of acetaminophen

Limit of detection (μM)	Linear dynamic range (μM)	Modifier	Electrode	Ref.
0.03	0.5–97	BiO nanorods	Screen printed electrode	42
0.051	0.09–7.0 and 16.4–1160	CeO_2 nanoparticles	Screen printed electrode	43
3.3×10^{-5}	10^{-4}–20	Electrodeposited graphene and zinc oxide nanocomposite	Glassy carbon electrode	44
4.29	10–1000	—	Graphite screen printed microelectrode arrays	45
0.03	0.09–35.0	Gold nanoparticles/multi-walled carbon nanotube	Glassy carbon electrode	46
0.45	10–125	Poly(4-amino-3-hydroxynaphthalene sulfonic acid)	Glassy carbon electrode	47
1.45	7–400	Graphene oxide-Y_2O_3 nanocomposite	Carbon paste electrode	48
0.009	0.025–35	Nitrogen-doped carbon nano-onions and gold nanoparticles	Glassy carbon electrode	49
0.005	0.009–325.0	Nanoparticle $[Co(5,5'\text{-dmbipy})_2(NCS)_2]$	Screen printed electrode	This work

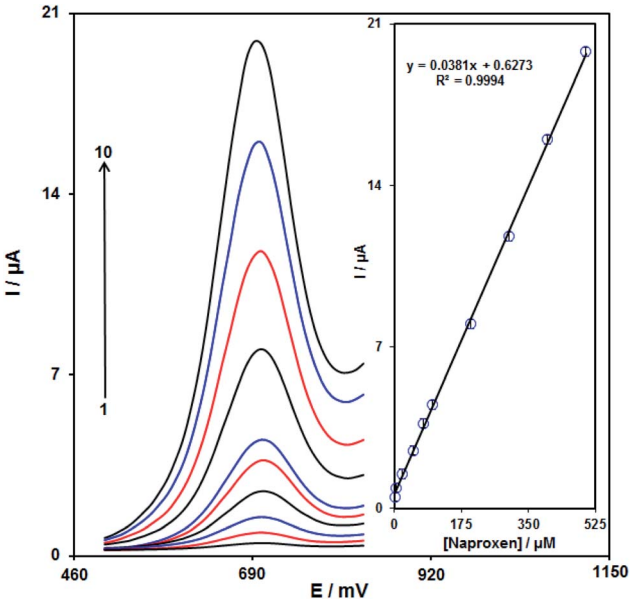

Fig. 12 DPVs of modified SPE in 0.1 M (pH 7.0) including various concentrations of naproxen. The curves 1–10 related to 1.0, 0.5, 20.0, 50.0, 75.0, 100.0, 200.0, 300.0, 400.0 and 500.0 μM of naproxen. Inset: plot of the current of peak like a function of concentration of naproxen material approximately in the 1.0–500.0.0 μM.

the time (s), and n is the number of electrons transferred. I values were plotted against $t^{-1/2}$ using the best fits related to various acetaminophen concentrations (Fig. 10a), and the plot of the slope of this straight line against acetaminophen concentrations are given in Fig. 10b. Using the slope related to the plot and Cottrell's equation the average value for acetaminophen's D was obtained to be 4.4 ($\pm$0.05) $\times$ 10^{-6} cm^2 s^{-1} which is comparable to some other electrochemical work (1.3 $\times$ 10^{-6} cm^2 s^{-1})[22] and CPE (4.97 $\times$ 10^{-6} cm^2 s^{-1}).[23]

3.3.4. DPV analysis and calibration plots. Using the peak currents of electrooxidation obtained by the modified SPE on differential pulse voltammetric analysis of various solutions of acetaminophen in 0.1 M PBS and according to the data (Fig. 11) (primary potential = 0.05 V, finish potential = 0.56 V, step potential = 0.002 V, modulation amplitude = 0.02505 V), the peak currents had a linear behavior against acetaminophen concentrations in the concentration approximately 0.009–325.0 μM (the value of correlation coefficient is 0.9999). The limit of detection at 3σ was determined to be 5.0 nM. Table 3 presents a comparison of electrochemical techniques for the finding of acetaminophen at the collected electrode in this research and some other researches.

In the case of naproxen peak, currents of naproxen oxidation at the modified SPE (Fig. 12) were linearly dependent on the naproxen amounts, in the range of 1.0 $\times$ 10^{-6} to 5.0 $\times$ 10^{-4} M

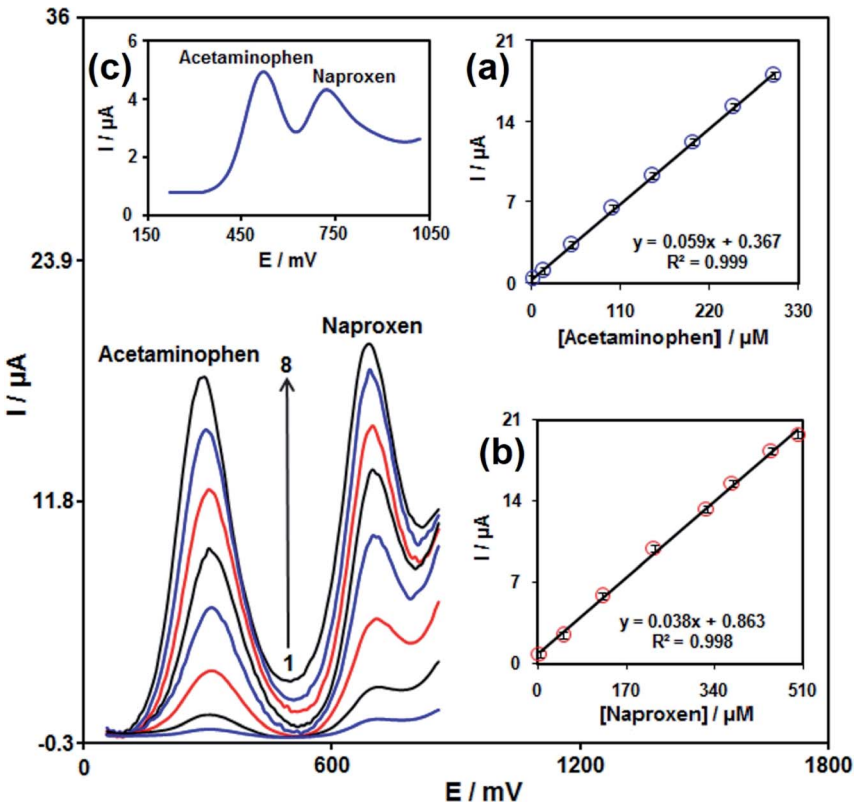

Fig. 13 DPVs of modified SPE in 0.1 M PBS (pH = 7.0) with diverse amounts of acetaminophen + naproxen. Curves 1–8 related to 0.5 + 5.0, 15.0 + 50.0, 50.0 + 125.0, 100.0 + 225.0, 150.0 + 325.0, 200.0 + 375.0, 250.0 + 450.0, and 300.0 + 500.0 μM of acetaminophen and naproxen. Insets: (a) plot of I_p against acetaminophen concentrations, (b) plot of I_p *versus* the amount of naproxen and (c) DPV of the unmodified SPE in 0.1 M PBS (pH = 7.0) with acetaminophen (300.0 μM) and naproxen (500.0 μM).

(with a value of correlation coefficient equal to 0.9994) (primary potential = 0.5 V, finish potential = 0.83 V, step potential = 0.002 V, modulation amplitude = 0.02505 V) and the limit of detection (3σ) was calculated 3.0×10^{-7} M.

3.3.5. Simultaneous detection of acetaminophen and naproxen. The DPV analyses were performed while simultaneously varying the amounts of acetaminophen and naproxen (primary potential = 0.05 V, finish potential = 0.86 V, step potential = 0.002 V, modulation amplitude = 0.02505 V) and the results included distinct respective anodic peaks at 300 and 710 mV for acetaminophen and naproxen (Fig. 13). It is notable that at the unmodified SPE distinct respective anodic peaks at 510 and 720 mV for acetaminophen and naproxen were observed in the inset C. This proves the applicability of the sensor for the simultaneous analysis of the species. The sensitivity of the analyses for acetaminophen was determined to be 0.059 μA μM^{-1}. This value was very close to that measured in pure acetaminophen solutions (0.060 μA μM^{-1}, see Section 3.3.4), containing the selectivity of the method.

3.3.6. The stability and repeatability of modified SPE. The response stability of modified SPE over time was investigated by using experimental in 14 days and in this period the electrodes were maintained in the situation of ambient.[50] It was found that the peak potentials of acetaminophen had constant, but the currents of electrooxidation had 2.6% as opposed to the initial amount.

To determine the antifouling characteristics of the modified SPE to the oxidation of acetaminophen and its oxidation products DPVs were obtained through the modified SPE in the presence of acetaminophen. The DPVs in the presence of acetaminophen sample was obtained after carrying out 15 cycles of potential at 50 mV s^{-1}. Albeit the potentials of peak did not alter; the electrooxidation currents illustrate a 2.4% decrease. The data displayed that not only does the sensitivity of the electrode rise, but also fouling effected using its oxidation product or the analyte reduces.

3.3.7. Real samples analysis. The approach of standard addition was applied for evaluating the applicability of the extended electrode to the analysis of acetaminophen and naproxen in real samples. The results of the tests on two samples are shown in Table 4 reflecting good recovery amounts for two species with amounts of acceptable relative standard deviation.

Table 4 The application of modified SPE for obtaining of acetaminophen and naproxen in acetaminophen tablet, naproxen tablet, and urine ($n = 5$). All concentrations are in μM

R.S.D. (%)		Recovery (%)		Found		Spiked		
NAP	AC	NAP	AC	NAP	AC	NAP	AC	Sample
—	3.2	—	—	—	4.0	0	0	Acetaminophen tablet
2.1	2.4	102.2	98.5	4.6	6.4	4.5	2.5	
1.8	2.7	101.8	97.3	5.6	7.3	5.5	3.5	
2.8	1.9	98.0	103.5	6.4	8.8	6.5	4.5	
3.4	2.4	98.7	98.9	7.4	9.4	7.5	5.5	
2.4	—	—	—	2.5	—	0	0	Naproxen tablet
3.5	1.7	101.5	98.0	6.6	4.9	4.0	5.0	
1.9	3.3	98.7	103.3	7.4	6.2	5.0	6.0	
2.5	2.2	97.6	102.8	8.3	7.2	6.0	7.0	
2.3	3.6	103.2	98.7	9.8	7.9	7.0	8.0	
—	—	—	—	—	—	0	0	Urine
2.4	3.2	98.0	102.5	4.9	4.1	5.0	4.0	
2.9	1.9	101.4	98.3	7.1	5.9	7.0	6.0	
3.4	2.7	103.3	97.5	9.3	7.8	9.0	8.0	
2.5	3.1	99.1	101.0	10.9	10.1	11.0	10.0	

4. Conclusions

In this work, we have shown the preparation of a new Co(II) compound with the formula [Co(5,5′-dmbpy)2(NCS)2] (**a1**). The compound (**a1**) was identified using FT-IR, UV-Vis spectroscopic techniques and elemental analysis, and single-crystal X-ray diffraction. The nano-size of compound (**a1**), has been synthesized using a sonochemical process. Nano-compound was distinguish using FT-IR, XRD, and SEM methods. A rapid, inexpensive, sensitive, and selective method for the designation of acetaminophen was presented based on electrocatalytic oxidation of the presented analytes on the modified SPE. The electrooxidation of acetaminophen at the modified SPE takes place at 300 mV. In the present study, the use of the modified SPE for the measurement of acetaminophen and naproxen simultaneously was demonstrated. The potential differences of 410 mV between acetaminophen and naproxen were large enough to distinguish acetaminophen and naproxen simultaneously and individually. Finally, the presented sensor applied to the designation of acetaminophen and naproxen in acetaminophen tablet, naproxen tablet, and urine with satisfactory recovery results. The high stability, wide linear range, reproducibility, and low detection limit, show that this sensor is an attractive candidate as a transducer for practical applications.

Conflicts of interest

The authors declare no competing interests.

Acknowledgements

The financial support provided by University of Sistan and Baluchestan and Kerman University of Medical Sciences is appreciated. This research was supported by National Research Foundation of Korea (NRF) funded by the Ministry of Science and ICT (2020M2D8A206983011). Furthermore, the financial supports of the Basic Science Research Program (2017R1A2B3009135) through the National Research Foundation of Korea is appreciated.

References

1 M. Ghalkhani and F. Ghorbani-Bidkorbeh, *Iran. J. Pharm. Res.*, 2019, **18**, 658.
2 M. R. Siddiqui, Z. A. AlOthman and N. Rahman, *Arabian J. Chem.*, 2017, **10**, S1409.
3 P. Mukherjee, A. Bagchi and A. Raha, *Afr. J. Pharm. Pharmacol.*, 2015, **9**, 834.

4 B. Kaur, R. Kumar, S. Chand, K. Singh and A. K. Malik, *Spectrochim. Acta, Part A*, 2019, **214**, 261.
5 N. Memon, T. Qureshi, M. I. Bhanger and M. I. Malik, *Curr. Anal. Chem.*, 2019, **15**, 349.
6 M. W. Lago, M. L. Friedrich, G. D. Iop, T. B. de Souza, P. de Azevedo Mello and A. I. H. Adams, *Talanta*, 2018, **181**, 182.
7 T. Hallaj, M. Amjadi, J. L. Manzoori and N. Azizi, *J. Lumin.*, 2017, **32**, 1174.
8 K. Zhang, T. H. Lee, H. Noh, O. K. Farha, H. W. Jang, J. W. Choi and M. Shokouhimehr, *Cryst. Growth Des.*, 2020, **19**, 7385.
9 V. K. Gupta, R. Jain, K. Radhapyari, N. Jadon and S. Agarwal, *Anal. Biochem.*, 2011, **408**, 179.
10 S. Tajik, H. Beitollahi, F. Garkani Nejad, M. Safaei, K. Zhang, Q. V. Le, R. S. Varma, H. W. Jang and M. Shokouhimehr, *RSC Adv.*, 2020, **10**, 21561.
11 S. Tajik, H. Beitollahi, S. Z. Mohammadi, M. Azimzadeh, K. Zhang, Q. V. Le, Y. Yamauchi, H. W. Jang and M. Shokouhimehr, *RSC Adv.*, 2020, **10**, 30481.
12 N. A. El-Maali, *Bioelectrochemistry*, 2004, **64**, 99.
13 A. Sakthivel, A. Chandrasekaran, S. Jayakumar, P. Manickam and S. Alwarappan, *J. Electrochem. Soc.*, 2019, **166**, B1461.
14 R. Güzel, H. Ekşi, E. Dinç and A. O. Solak, *J. Electrochem. Soc.*, 2013, **160**, B119.
15 M. A. Khandkar, D. V Parmar, M. Das and S. S. Katyare, *J. Pharm. Pharmacol.*, 1996, **48**, 437.
16 R. N. Brogden, R. C. Heel, T. M. Speight and G. S. Avery, *Drugs*, 1979, **18**, 241.
17 H. F. Miranda, M. M. Puig, J. C. Prieto and G. Pinardi, *Pain*, 2006, **121**, 22.
18 P. Seideman, P. Samuelson and G. Neander, *Acta Orthop. Scand.*, 1993, **64**, 285.
19 P. Seideman, *Int. J. Rheumatol.*, 1993, **32**, 1077.
20 H. Mahmoudi-Moghaddam, H. Beitollahi, S. Tajik and H. Soltani, *Electroanalysis*, 2015, **27**, 2620.
21 H. Beitollahi, H. Karimi-Maleh and H. Khabazzadeh, *Anal. Chem.*, 2008, **80**, 9848.
22 S. Tajik, H. Beitollahi, F. Sheikh Shoaie, M. A. Khalilzadeh, M. Shahedi Asl, Q. V. Le, K. Zhang, H. W. Jang and M. Shokouhimehr, *RSC Adv.*, 2020, **10**, 37834.
23 S. F. Wang, F. Xie and R. F. Hu, *Sens. Actuators, B*, 2007, **123**, 495.
24 M. M. Foroughi, H. Beitollahi, S. Tajik, M. Hamzavi and H. Parvan, *Int. J. Electrochem. Sci.*, 2014, **9**, 2955.
25 T. W. Chen, U. Rajaji, S. M. Chen, S. Chinnapaiyan and R. J. Ramalingam, *Ultrason. Sonochem.*, 2019, **56**, 430.
26 M. M. Foroughi, H. Beitollahi, S. Tajik, A. Akbari and R. Hosseinzadeh, *Int. J. Electrochem. Sci.*, 2014, **9**, 8407.
27 G. G. Gerent and A. Spinelli, *J. Hazard. Mater.*, 2017, **330**, 105.
28 M. Govindasamy, S. Sakthinathan, S. M. Chen, T. W. Chiu, A. Sathiyan and J. P. Merlin, *Electroanalysis*, 2017, **29**, 1950.
29 A. Ourari, B. Ketfi, S. I. R. Malha and A. Amine, *J. Electroanal. Chem.*, 2017, **797**, 31.
30 S. G. Leonardi, D. Aloisio, N. Donato, S. Rathi, K. Ghosh and G. Neri, *Mater*, 2014, **133**, 232.
31 M. Amiri, Z. Pakdel, A. Bezaatpour and S. Shahrokhian, *Bioelectrochemistry*, 2011, **81**, 81.
32 M. R. Ganjali, F. Garkani-Nejad, S. Tajik, H. Beitollahi, E. Pourbasheer and B. Larijanii, *Int. J. Electrochem. Sci.*, 2017, **12**, 9972.
33 H. Wang, Y. Duan, G. Zhao, Z. Wang and G. Liu, *Int. J. Electrochem. Sci.*, 2015, **10**, 8759.
34 A. Economou, *Sensors*, 2018, **18**, 1032.
35 T. Kondori, O. Shahraki, N. Akbarzadeh-Torbati and Z. Aramesh-Boroujeni, *J. Biomol. Struct. Dyn.*, 2020, DOI: 10.1080/07391102.2020.1713893.
36 T. Kondori, N. Akbarzadeh-Torbati, M. Dušek and V. Eigner, *Chem. Pap.*, 2019, **73**, 1639.
37 T. Kondori, N. Akbarzadeh-Torbati and C. Graiff, *J. Iran. Chem. Soc.*, 2019, **16**, 1827.
38 R. Alizadeh and V. Amani, *J. Struct. Chem.*, 2013, **22**, 1153.
39 T. Kondori, N. Akbarzadeh-Torbati, K. Abdi, M. Dušek and V. Eigner, *J. Biomol. Struct. Dyn.*, 2020, **38**, 236–247.
40 M. Lalia-Kantouri, Ch. D. Papadopoulos, M. Quiros and A. G. Hatzidimitriou, *Synth. React. Inorg., Met.-Org., Nano-Met. Chem.*, 2007, **26**, 1292.
41 A. J. Bard and L. R. Faulkner, *Electrochemical Methods Fundamentals and Applications*, Wiley, New York, 2nd edn, 2001.
42 B. G. Mahmoud, M. Khairy, F. A. Rashwan and C. E. Banks, *Anal. Chem.*, 2017, **89**, 2170.
43 M. Khairy, B. G. Mahmoud and C. E. Banks, *Sens. Actuators, B*, 2018, **259**, 142.
44 L. Jiang, S. Gu, Y. Ding, F. Jiang and Z. Zhang, *Nanoscale*, 2014, **6**, 207.
45 F. Tan, J. P. Metters and C. E. Banks, *Sens. Actuators, B*, 2013, **181**, 454.
46 T. Madrakian, E. Haghshenas and A. Afkhami, *Sens. Actuators, B*, 2014, **193**, 451.
47 M. Tefera, A. Geto, M. Tessema and S. Admassie, *Food Chem.*, 2016, **210**, 156.
48 C. Martínez-Sánchez, F. Montiel-González and V. Rodríguez-González, *J. Taiwan Inst. Chem. Eng.*, 2019, **96**, 382.
49 E. Sohouli, F. Shahdost-Fard, M. Rahimi-Nasrabadi, M. E. Plonska-Brzezinska and F. Ahmadi, *J. Electroanal. Chem.*, 2020, **871**, 114309.
50 S. Tajik, H. Beitollahi, F. Garkani Nejad, K. O. Kirlikovali, Q. V. Le, H. W. Jang, R. S. Varma, O. K. Farha and M. Shokouhimehr, *Cryst. Growth Des.*, 2020, **20**, 7034.